

Tocilizumab treatment in severe COVID-19 patients attenuates the inflammatory storm incited by monocyte centric immune interactions revealed by single-cell analysis

Chuang Guo^{1,7}, Bin Li^{1,7}, Huan Ma¹, Xiaofang Wang², Pengfei Cai¹, Qiaoni Yu¹, Lin Zhu¹, Liying Jin¹, Chen Jiang¹, Jingwen Fang³, Qian Liu¹, Dandan Zong¹, Wen Zhang¹, Yichen Lu¹, Kun Li¹, Xuyuan Gao¹, Binqing Fu^{1,4}, Lianxin Liu², Xiaoling Ma⁵, Jianping Weng⁶, Haiming Wei^{1,4}, Tengchuan Jin^{1,4,†}, Jun Lin^{1,4,†}, Kun Qu^{1,4,†}

¹Department of oncology, The First Affiliated Hospital of USTC, Division of Molecular Medicine, Hefei National Laboratory for Physical Sciences at Microscale, Division of Life Sciences and Medicine, University of Science and Technology of China, Hefei, Anhui, 230021, China.

²Department of Hepatobiliary Surgery, the First Affiliated Hospital of USTC, Division of Life Sciences and Medicine, University of Science and Technology of China, Hefei, Anhui, 230021, China.

³HanGene Biotech, Xiaoshan Innovation Polis, Hangzhou, Zhejiang, China

⁴CAS Center for Excellence in Molecular Cell Sciences, the CAS Key Laboratory of Innate Immunity and Chronic Disease, University of Science and Technology of China, Hefei, Anhui, 230027, China.

⁵Department of Laboratory Medicine, The First Affiliated Hospital of USTC, Division of Life Sciences and Medicine, University of Science and Technology of China, Hefei, Anhui, 230001, China

⁶Department of Endocrinology and Metabolism, The First Affiliated Hospital of USTC, Division of Life Sciences of Medicine, University of Science and Technology of China, Hefei 230026, China.

⁷These authors contributed equally to this work.

†Corresponding should be addressed to Kun Qu (qukun@ustc.edu.cn).

Jun Lin (linjun7@ustc.edu.cn); Tengchuan Jin (jint@ustc.edu.cn)

Contact Information:

Kun Qu, Ph.D.

Division of Molecular Medicine, Hefei National Laboratory for Physical Sciences at Microscale, Division of Life Sciences and Medicine, University of Science and Technology of China, Hefei, Anhui, 230027, China.

Email: qukun@ustc.edu.cn

Phone: +86-551-63606257

ABSTRACT

Coronavirus disease 2019 (COVID-19) has caused more than 40,000 deaths worldwide¹. Approximately 14% of patients with COVID-19 experienced severe disease and 5% were critically ill². Studies have shown that dysregulation of the COVID-19 patients' immune system may lead to inflammatory storm and cause severe illness and even death^{3,4}. Tocilizumab treatment targeting interleukin 6 receptor has shown inspiring clinical results of severe COVID-19 patients⁵. However, the immune network with Tocilizumab treatment at single cell resolution has not been uncovered. Here, we profiled the single-cell transcriptomes of 13,289 peripheral blood mononuclear cells isolated at three longitudinal stages from two severe COVID-19 patients treated with Tocilizumab. We identified a severe stage-specific monocyte subpopulation and these cells centric immune cell interaction network connected by the inflammatory cytokines and their receptors. The over-activated inflammatory immune response was attenuated after Tocilizumab treatment, yet immune cells including plasma B cells and CD8⁺ T cells still exhibited an intense humoral and cell-mediated anti-virus immune response in recovered COVID-19 patients. These results provided critical insights into the immunopathogenesis of severe COVID-19 and revealed fundamentals of effectiveness in Tocilizumab treatment.

Keywords : Coronavirus disease 2019 (COVID-19); Severe acute respiratory syndrome coronavirus 2 (SARS-CoV-2); Tocilizumab; Single-cell RNA sequencing (scRNA-seq); Inflammatory storm; Monocyte

Main

As of Apr 1, 2020, WHO reported 40,598 deaths out of 823,626 confirmed cases infected by severe acute respiratory syndrome coronavirus 2 (SARS-CoV-2), and these numbers are still growing rapidly¹. Approximately 14% of patients with COVID-19 experienced severe disease, and 5% were critically ill suffered from 49% fatality rate², which may be caused by patients' abnormal immune system activation^{3,4,6}. Hence, there is an urgent need for researchers to understand how the immune system respond to the viral infections at severe stage and thereby provide effective treatment strategies.

Studies have shown that the inflammatory storm caused by excessive immune responses was associated with the crucial cause for mortality in COVID-19^{7,8}. Plasma concentrations of a series of inflammatory cytokines, such as granulocyte-macrophage colony-stimulating factor (GM-CSF), interleukin (IL)-6⁴, tumor necrosis factor α (TNF- α), IL-2, 7, 10 and granulocyte colony-stimulating factor (G-CSF)⁹ were increased after SARS-CoV-2 infections. Further investigation demonstrated peripheral inflammatory monocytes and pathogenic T cells may incite cytokine storm in severe COVID-19 patients^{4,7}. To calming inflammatory storm, Tocilizumab, which targeting IL-6 receptors and has proved its effectiveness in the treatment of cytokine release syndrome that is severe or life-threatening^{10,11}, was used in the treatment of severe COVID-19. After receiving Tocilizumab, the body temperature of the patients returned to normal after 24 hours. The concentration of oxygen inhalation was significantly decreased on the 5th day⁵. However, the immune network arousing the inflammatory storm in severe or recovery stage during Tocilizumab therapy at single cell level has not been uncovered.

Here, we profiled the peripheral immune cells of COVID-19 patients using single-cell transcriptome sequencing. We obtained 5 peripheral blood samples from 2 severe COVID-19 patients at 3 consecutive time-points from the severe to recovery stages during Tocilizumab treatment (Fig. 1a). Specifically, the blood samples at severe stage were collected within 12 hours of Tocilizumab was given. The blood samples at recovery stage were collected at the 5th and 7th day after Tocilizumab treatment. The

patients at severe stage had decreased number of lymphocytes, increased percentage of neutrophil and concentrations of C-reaction protein, and increased expression of IL-6 (Supplementary Table 1). Peripheral blood mononuclear cells (PBMCs) were isolated and subjected to single-cell mRNA sequencing (scRNA-seq) using the 10X platform (Fig. 1a, Supplementary Table 2). After filtering low quality cells, we retained a total of 13,289 single transcriptomes of PBMCs. Of these, 4,364 cells were from severe stage and 8,925 were from patients at recovery stage.

To investigate the heterogeneity and differences of PBMCs between COVID-19 patients and healthy controls, we integrated our COVID-19 single cell transcriptomes with the published single-cell profiles of healthy PBMC from the 10X official website¹² and obtained a total of 69,237 cells (See **Methods**) (Fig. 1b-d). We then applied Seurat¹³ to normalize and cluster the gene expression matrix, and identified 20 unique cell subsets, which were visualized via uniform manifold approximation and projection (UMAP) (Fig. 1b-d). Cell lineages, including monocytes, CD4⁺ and CD8⁺ T, $\gamma\delta$ T, NK, B, plasma B and myeloid dendritic cells (mDC), plasmacytoid dendritic cells (pDC), platelet and CD34⁺ progenitor cells were identified based on the expression of known marker genes (Fig. 1e, Extended Data Fig.1a). With that, we delineated the landscape of circulating immune cells in severe COVID-19 patients.

We next explored the distribution of immune cells from the severe, recovery and healthy stage in each cell subpopulation (Fig. 1f, Extended Data Fig.1b). We observed that a monocyte subpopulation (cluster 9) existed only in patients at severe stage. Plasma B cells (cluster 11), effector CD8⁺ T (cluster 6), proliferative MKI67⁺CD8⁺ T cells (cluster 12) and NK cells (cluster 7) were significantly enriched in patients versus control. However, a number of subpopulations, such as $\gamma\delta$ T cells (cluster 8), pDCs (cluster 15) and mDCs (cluster 10 and 19), most monocytes (cluster 2, 13 and 14) existed only in patients at recovery stage and healthy controls, indicating that these cell types gradually become normal after the treatment. No significant differences were observed in CD4⁺ T (cluster 1 and 4), naïve CD8⁺ T (cluster 3) and B cells (cluster 5)

in patients versus control.

Monocytes were reported to play a vital role in CAR-T induced cytokine-release syndrome¹⁴ and SARS-CoV-2 infection caused inflammatory storm⁴, therefore we explored the features and functions of the monocyte from COVID-19 patients. We detected 1,737 monocytes in patients, 927 from severe stage and 810 from recovery stage, and integrated 9,787 monocytes from health control. The UMAP plot displayed two main clouds of monocytes that were clearly segregated (Fig 2a). One monocyte subpopulation (cluster 9) was almost exclusively consisted of cells from severe stage and others (cluster 2, 13, 14, 17) were dominated by cells from the recovery and healthy stages (Fig 2b), suggesting a severe-stage specific monocyte subpopulation.

We then investigated the expressions of several selected inflammatory cytokines and observed that these genes were all significantly enriched in severe stage-specific monocytes (Fig. 2c, $P < 0.001$, Wilcoxon rank-sum test). To further explore the transcriptional differences among the monocytes' subtypes, we performed a pairwise comparison of the gene expressions in severe, recovery and healthy stages. We obtained 2,335 differentially expressed genes (DEGs) enriched in each stage, within which reported cytokine storm related genes, such as *TNF*⁹, *IL10*⁹, *CCL3*⁹ and *IL6*⁴ were found significantly higher expressed in severe stage-specific monocytes (Fig 2d, Supplementary Table 3). In addition, we also discovered a large number of significant and inflammatory related genes that were less reported (Fig 2d, fold change > 2 , $P < 10^{-3}$), including chemokine genes *CCL4*, *CCL20*, *CXCL2*, *CXCL8* and *CXCL9*, inflammasome activation associated genes *NLRP3* and *IL1B*, and complement pathway genes *CIQA*, *CIQB* and *CIQC* (Extended Data Fig.2a-c, Supplementary Table 4). These results indicated that this monocyte subpopulation may contribute to the inflammatory storm in severe COVID-19 patients.

We also observed that genes involved in “acute inflammatory response” and “leukocyte chemotaxis” were significantly decreased at recovery and healthy stage (Fig.2e, f, Supplementary Table 5), suggesting that the inflammatory storm caused by

this monocyte subpopulation was suppressed after the Tocilizumab treatment.

Next, we explored the transcription factors (TFs) that may be involved in the regulation of inflammatory storm in monocytes. We used SCENIC¹⁵ and predicted 15 TFs that may regulate genes which were enriched in severe stage-specific monocyte (Fig 2g). By constructing a gene regulatory network, we found 3 of them, namely *ETS2*, *NFIL3* and *PHLDA2* were regulating the cytokine storm relevant genes (Extended Data Fig.2d). In addition, we found the expressions of *ETS2*, *NFIL3* and *PHLDA2* and their target genes were enhanced in severe-specific monocyte subpopulation (Fig 2h), suggesting these 3 TFs may regulate the inflammatory storm in monocytes.

Given that monocytes in the severe stage may be involved in the regulation of a variety of immune cell types, we used the accumulated ligand/receptor interaction database¹⁶ CellPhoneDB (www.cellphonedb.org) to identify alterations of molecular interactions between monocytes and all the immune cell subsets (Supplementary Table 6). We found 15 pairs of cytokines and their receptors whose interaction were significantly altered in severe versus recovery and healthy stages (Fig 3a). Consistent with previous study⁴, we found monocytes interacted with CD4⁺ T cells and plasma B cells in patients at severe stage through the ligand/receptor pairs of IL-6/IL-6R. This interaction, together with many other cytokine storm relevant cell-cell communications were then extensively attenuated after the treatment of Tocilizumab (Fig 3b), suggesting that this drug may functioning by effectively blocking the inflammatory storm in severe COVID-19 patients.

In addition, we also discovered many other ligand/receptor pairs involved in a broader spectrum of immune cell communications enriched at the severe stage. For example, TNF- α and its receptors, which connected monocytes with many other immune cells. Others like IL-1 β and its receptor, which connected monocytes with CD8⁺ T cells. Chemokines, such as CCL4L2, CCL3 and CCL4 and their receptors were also found enriched at severe stage. These cytokines and their receptors may serve as potential drug targets to treat COVID-19 patients at severe stage, and some of their

inhibitors are undergoing clinical trials in multiple places around the world (Supplementary Table 7). Collectively, these findings illustrated the molecular basis of cell-cell interactions at the peripheral blood of COVID-19 patients, leading to a better understanding of the mechanisms of inflammatory storm of the disease.

Robust multi-factorial immune responses can be elicited against viral infection, such as avian H7N9 disease^{17,18}. A recent report has found effective immune responses from a non-severe COVID-19 patient¹⁹. However, it is not clear whether the anti-virus immune response would be affected after Tocilizumab treatment. Therefore, the anti-virus immune responses from the humoral and cell-mediated immunity in COVID-19 patients at severe stage were compared with recovery stage and healthy controls. As expected, we found plasma B cells were barely existing in healthy controls (Fig. 4a). By contrast, significantly higher proportion of plasma B cells was exclusively increased in both severe and recovery stages (Fig. 4a, b), suggesting powerful anti-virus humoral immune responses during Tocilizumab treatment.

CD8⁺ T cells are a critical component of cell-mediated immunity against viral infections by killing infected cells and secreting proinflammatory cytokines. To identify the anti-virus immune responses from the cell-mediated immunity during Tocilizumab treatment, we detected 12,121 CD8⁺ T cells from our analysis. Clustering these cells revealed 3 subtypes: naïve CD8⁺ T cells (cluster 3), effector CD8⁺ T cells (cluster 6) and a subset of CD8⁺ T cells with proliferation characteristics (cluster 12) (Fig. 4c, d). Among them, the cells from the severe patients were mainly distributed in the effector CD8⁺ T cell cluster (Fig. 4c, d). We then conducted pairwise comparisons to identify DEGs of CD8⁺ T cells between the severe, recovery and healthy stages (Fig. 4e, Supplementary Table 8). We found that genes enriched in severe stage showed “regulation of cell activation” signatures (Fig. 4f, Supplementary Table 9; $P < 10^{-10}$). Meanwhile, genes involved in “leukocyte mediated cytotoxicity” and “positive regulation of cytokine production” were highly enriched in CD8⁺ T cells from COVID-19 patients at both severe and recovery stage (Fig. 4g, Supplementary Table 9; $P < 10^{-10}$).

5). We further detected elevated expression of the 108 and 449 genes involved in these GO terms (Fig. 4h, i, Supplementary Table 10). Together, these results demonstrated the critical evidence that robust adaptive immune responses against SARS-CoV-2 infection exist in severe stage and remain after Tocilizumab treatment.

The immune system is crucial to fight off viral infection^{20,21}. Recent studies have illustrated that monocytes may be the main cause of exacerbation and even death of COVID-19 patients through inflammatory storms⁴. In this study, we discovered a specific monocyte subpopulation that may lead to the inflammatory storm in patients at severe stage through single-cell mRNA sequencing. By analyzing the monocyte-centric ligand/receptor interactions, we revealed a severe stage-specific landscape of peripheral immune cell communication that may drive the inflammatory storm in COVID-19 patients. With that we obtained a list of cytokine storm relevant ligand/receptors that can serve as candidate drug targets to treat the disease, and provided mechanistic insights of the immunopathogenesis of COVID-19.

There are always questions about whether Tocilizumab treatment may affect the antiviral effect of the body^{22,23}. Our single cell profiles illustrated a sustained humoral and cell-mediated anti-virus immune response of COVID-19 patients at both severe and recovery stage. For example, the proportion of plasma B cells with antibody-secreting function were keeping at high levels and the cytotoxicity and cytokine production of effector CD8⁺ T cells were also remained stable in severe COVID-19 patients after Tocilizumab treatment.

The distributions of NK cells were significantly different in the two patients (Extended Data Fig.1b), and the analysis of gene expression differences did not enrich significant biological functions, therefore we did not discuss them in depth. The normal functions of other cell types, such as $\gamma\delta$ T cells and DCs, were almost lost under severe conditions, and the contribution of these cells to the progression of the disease requires further investigation.

Methods

Human samples

Peripheral blood samples were obtained from two severe COVID-19 patients. The patient severity was defined by the "Diagnosis and Treatment of COVID-19 (Trial Version 6)" which was released by The General Office of the National Health Commission and the Office of the National Administration of Traditional Chinese Medicine. Patient PZ was defined as a severe patient for his peripheral capillary oxygen saturation (SPO₂) <93%. Patient PZ provided 2 blood samples at severe stage (Day 1) and recovery stage (Day 5). Patient PW was defined as critical ill for respiratory failure, multiple organ dysfunction (MOD) and SPO₂ <93% under high flow oxygen (50 L/min, FIO₂ 50%). Patient PW provided 3 blood samples at severe stage (Day 1) and recovery stage (Day 5 and Day 7). All samples were collected from the First Affiliated Hospital of University of Science and Technology of China. Before blood draw, informed consent was obtained from each patient. Ethical approvals were obtained from the ethics committee of the First Affiliated Hospital of the University of Science and Technology of China (No. 2020-XG(H)-020).

Cell Isolation

We collected 2ml peripheral blood each time from the COVID-19 patients. Peripheral blood mononuclear cells (PBMC) were freshly isolated from the whole blood by using a density gradient centrifugation using Ficoll-Paque and cryopreserved for subsequent generation of single-cell RNA library.

Single-cell RNA-seq

We generated single-cell transcriptome library following the instructions of single-cell 3' solution v2 reagent kit (10x Genomics). Briefly, after thawing, washing and counting cells, we loaded the cell suspensions onto a chromium single-cell chip along with partitioning oil, reverse transcription (RT) reagents, and a collection of gel beads that

contain 3,500,000 unique 10X Barcodes. After generation of single-cell gel bead-in-emulsions (GEMs), RT was performed using a C1000 TouchTM Thermal Cycler (Bio-Rad). The amplified cDNA was purified with SPRIselect beads (Beckman Coulter). Single-cell libraries were then constructed following fragmentation, end repair, polyA-tailing, adaptor ligation, and size selection based on the manufacturer's standard parameters. Each sequencing library was generated with unique sample index. Libraries were sequenced on the Illumina NovaSeq 6000 system.

Single-cell RNA-seq data processing

The raw sequencing data of patients and health donors were processed using Cell Ranger (version 3.1.0) against the GRCh38 human reference genome with default parameters, and data from different patients and disease stages were combined by the Cell Ranger 'aggr' function. We are uploading the scRNA-seq data of PBMCs from the 2 severe COVID-19 patients to the Genome Sequence Archive at BIG Data Center and the accession number will be available upon request. We also used the scRNA-seq data of PBMCs from 2 healthy donors, which can be downloaded from the 10X genomics official website. Firstly, we filtered low quality cells using Seurat¹³ (version 3.1.4). For cells from COVID-19 patients (PZ and PW), we retained cells with detected gene numbers between 500 and 6,000 and mitochondrial UMIs less than 10%. For cells from healthy donors, we retained cells with detected gene numbers between 300 and 5,000 and mitochondrial UMIs less than 10%. Subsequently we normalized gene counts for each cell using the "NormalizeData" function of Seurat with default parameters.

In downstream data processing, we used canonical correlation analysis (CCA) and the top 40 canonical components to find the "anchor" cells between patients and healthy controls. We then used the "IntegrateData" function in Seurat to integrate all the cells. We clustered cells based on the integrated dataset using Seurat with parameter "resolution=0.3" and generated 20 clusters. To display cells in a 2-dimensional space, we ran the principal component analysis (PCA) on the integrated dataset and adopted

the first 50 principal components for the uniform manifold approximation and projection (UMAP) analysis.

Differential expression analysis

To search for the differentially expressed genes (DEGs), we first assign the negative elements in the integrated expression matrix to zero. We used Wilcoxon rank-sum test to search for the DEGs between each pair of the 3 stages of cells (i.e. severe stage, recovery stage and healthy control). We applied multiple thresholds to screen for DEGs, including mean fold-change >2, *P* value <0.001, and were detected in >10% of cells in at least one stage.

We defined stage A specific-DEGs as the intersections between the DEGs in stage A versus stage B and the DEGs in stage A versus stage C. We defined stage A and B common-DEGs as the intersections of the DEGs in stage A versus stage C and the DEGs in the stage B versus stage C, minus the DEGs between stage A and B. In this way, we obtained the specific-DEGs for each stage, and the common-DEGs for each pair of the 3 stages. We then uploaded these DEG groups to the Metascape²⁴ website (<https://metascape.org/gp/index.html#/main/step1>), and used the default parameters to perform Gene Ontology (GO) analysis for each stage.

Motif enrichment and regulatory network

We adopted SCENIC¹⁵ (version 1.1.2) and RcisTarget database to build the gene regulatory network of CD14⁺ monocytes. Since the number of CD14⁺ monocytes from healthy control (N = 9,618) was more than those from the severe and recovery stages (N = 1,607), to balance their contributions in the motif analysis, we randomly sampled 2,000 CD14⁺ monocytes from the healthy control for calculation. We selected 13,344 genes that were detected in at least 100 monocytes or included in the DEGs of the 3 stages as the input features for SCENIC. With default parameters, SCENIC generated the enrichment scores of 427 motifs. We used the student's t-test to calculate the *P*

values of these motifs between severe stage and healthy control, and selected severe-specific enriched motifs with fold change >1.5 and P value $< 10^{-100}$.

We then applied the enrichment scores of the severe-specific enriched motifs and the expressions of their targeted genes to Cytoscape²⁵ to construct a connection map for the gene regulatory network, as shown in Extended Data Fig. 2b. The thickness of line connecting TFs and target genes represented the weight of regulatory link predicted by SCENIC.

Ligand/receptor interaction analysis

To identify potential cellular communications between monocytes and other cell types (CD4⁺ T, CD8⁺ T, B, plasma B and NK cells), we applied the CellphoneDB¹⁶ algorithm to the scRNA-seq profiles from the severe, recovery and healthy stages. CellphoneDB evaluated the impact of a ligand/receptor interactions based on the ligand expression in one cell type and its corresponding receptor expression in another cell type. To identify the enriched ligand/receptor interactions in patients at severe stage, we selected the ligand/receptor interactions with more significant (P value < 0.05) cell-cell interaction pairs in the severe stage than that in the recovery and healthy stages. We also included ligand/receptor pairs which were highly expressed in severe stage.

Data Availability

We are uploading the scRNA-seq data of PBMCs from the 2 severe COVID-19 patients to the Genome Sequence Archive at BIG Data Center and the accession number will be available upon request. We also used the scRNA-seq data of PBMCs from 2 healthy donors, which can be downloaded from the 10X genomics official website.

Acknowledgements

Funding: This work was supported by the National Key R&D Program of China (2017YFA0102900 to K.Q.), the National Natural Science Foundation of China grants

(81788101, 31970858, 31771428, 91940306 and 91640113 to K.Q., 31700796 to C.G. and 81871479 to J.L.), the Fundamental Research Funds for the Central Universities (to K.Q.). We thank the USTC supercomputing center and the School of Life Science Bioinformatics Center for providing supercomputing resources for this project.

Author Contributions

K.Q. conceived and supervised the project; K.Q., C.G. and J.L. designed the experiments; C.G. and J.L. performed the experiments and conducted all the sample preparation for NGS with the help from H.M. and T.C.; B.L. performed the data analysis with the help from P.C., Q.Y., L.Z., L.J., C.J., Q.L., D.Z., W.Z., Y.L., K.L., X.G. and J.F.; T.C., X.W., L.L. and X.M. provided COVID-19 blood samples and clinical information. K.Q., C.G., J.L. and B.L. wrote the manuscript with the help of B.F., H.W. and all the other authors.

Competing interests

Jingwen Fang is the chief executive officer of HanGen Biotech.

Figure Legends

Figure 1 | An atlas of peripheral immune cells in severe COVID-19 patients. a, Flowchart depicting the overall design of the study. Blood draws from patient PZ were performed at 2 time points (Day1 and Day5), and PW at 3 time points (Day1, Day5, and Day7). Patients at Day 1 were at severe stage and Day 5 and Day 7 were at recovery stages. Samples were collected within 12 hours of Tocilizumab was given at Day 1. **b-d,** UMAP representations of single-cell transcriptomes of 13,289 PBMCs. Cells are color-coded by clusters (**b**), disease stages (**c**), and the corresponding patient or healthy control (**d**). Dotted circles represented cell types with > 5% proportion of PBMCs in (**b**) and clusters significantly enriched in patients versus control in (**c, d**). Mono, monocyte; NK, natural killer cells; mDC, myeloid dendritic cells; pDC, plasmacytoid dendritic

cells. **e**, Violin plots of selected marker genes (upper row) for multiple cell subpopulations. The left column are cell subtypes identified by combination of marker genes. **f**, Bar chart showing the proportion of immune cells from the severe, recovery and healthy stage in each cell subpopulation.

Figure 2 | A unique monocyte subpopulation contributes to the inflammatory

storm in COVID-19 patients at severe stage. a, UMAP plot showing 4 clusters of

CD14⁺ monocytes and 1 cluster of CD16⁺ monocyte. Cells are color-coded by clusters.

b, Bar plot of the proportion of monocytes in cluster 9 at the severe, recovery and

healthy stages. **c**, UMAP plots showing the expressions of selected cytokines in all

monocytes clusters. **d**, Heatmap of differentially expressed genes (DEGs) in monocytes

from pairwise comparison between severe, recovery and healthy stages. **e,f**, Box plot

of the average expressions of genes involved in the signaling pathway "Acute

inflammatory response" and "Leukocyte chemotaxis" in monocytes from severe,

recovery and healthy stages. Center line, median; box limits, upper and lower quartiles;

whiskers, 1.5x interquartile range; points, outliers; **** represents P value $< 10^{-100}$,

student's t-test. **g**, Heatmap of the area under the curve (AUC) scores of expression

regulation by transcription factors (TFs) estimated using SCENIC. Shown are the top

differential TFs. **h**, UMAP plots showing the expressions of genes *ETS2*, *NFIL3* and

PHLDA2 in monocytes (top) and the AUC of the estimated regulon activity of the

corresponding TFs, indicating the degree of expression regulation of their target genes

(bottom).

Figure 3 | The monocyte-centric molecular interactions of peripheral immune cells

in COVID-19 patients at severe stage. a, Dot plot of predicted interactions between

monocytes and indicated immune cell types in the severe, recovery and healthy stages.

P values were measured by circle sizes. The expression levels of the interacted genes

were indicated by colors, scales on the right. **b**, Summary illustration depicting the

cytokine/receptor interactions between monocytes and other types of peripheral immune cells in severe, recovery and healthy stages. Bolder lines indicated predicted enriched ligand/receptor interactions between monocytes and other immune cell types.

Figure 4 | Enhanced humoral and cell-mediated immunity in severe COVID-19

patients. a, UMAP representations of B and plasma B cell clusters from the severe, recovery and healthy stages. **b**, Bar plot of the proportions of plasma B cells in B cell lineage from severe, recovery and healthy stages. **c**, UMAP representations of CD8⁺ T cell subtypes (left) and the distribution of cells from severe, recovery and healthy stages in each subtype (right). **d**, Dot plot of the expression of *CCR7*, *PRDM1* and *MKI67* in all CD8⁺ T cell subtypes. **e**, Heatmap of differentially expressed genes in effector CD8⁺ T cells from pairwise comparison between the severe, recovery and healthy stages. **f, g**, Bar plots of GO terms enriched in effector CD8⁺ T cells from the severe stage (**f**) or severe and recovery stages (**g**). **h, i**, Box plots of the average expressions of genes involved in the signaling pathway "Leukocyte mediated cytotoxicity" and "Positive regulation of cytokine production" in the effector CD8⁺ T cells from severe stage, recovery stage and healthy controls. Center line, median; box limits, upper and lower quartiles; whiskers, 1.5x interquartile range; points, outliers; **** represents *P* value < 10⁻³⁰.

Extended Data Figure Legends and Supplementary Tables

Extended Data Figure 1 | Identification of single-cell subpopulations. a, UMAP plots showing the expressions of selected marker genes in all identified cells. **b**, Bar chart showing the percentage of cell subpopulations in different clinical stages of patients and healthy controls.

Extended Data Figure 2 | Features of monocyte subpopulations. a-c, Bar plots of enriched GO terms of genes highly expressed in monocytes at severe stage (**a**), severe

and recovery stages **(b)**, and healthy controls **(c)**. **d**, Severe stage specific monocyte regulatory network predicted by SCENIC. Transcription factors were shown in rectangles and their target genes in circles.

Supplementary Table 1 | Baseline characteristics and laboratory findings of COVID-19 patients in this study.

Supplementary Table 2 | Sequencing data quality.

Supplementary Table 3 | DEGs of different stages of CD14 monocytes.

Supplementary Table 4 | GOterms of DEGs of CD14 monocytes.

Supplementary Table 5 | Gene sets of GO terms in Figure 2e and 2f.

Supplementary Table 6 | Interactions of cytokines and receptors in different stages.

Supplementary Table 7 | Drugs for targeting cytokines or their receptors.

Supplementary Table 8 | DEGs of different stages of effector CD8 T cells.

Supplementary Table 9 | GOterms of DEGs of effector CD8 T cells.

Supplementary Table 10 | Gene sets of GO terms in Figure 4h and 4i.

Reference:

- 1 WHO. Coronavirus disease 2019 (COVID-19) Situation Report - 72. (2020).
- 2 Wu, Z. & McGoogan, J. M. Characteristics of and Important Lessons From the Coronavirus Disease 2019 (COVID-19) Outbreak in China: Summary of a Report of 72314 Cases From the Chinese Center for Disease Control and Prevention. *JAMA*, doi:10.1001/jama.2020.2648 (2020).
- 3 Mehta, P. *et al.* COVID-19: consider cytokine storm syndromes and immunosuppression. *Lancet* **395**, 1033-1034, doi:10.1016/S0140-6736(20)30628-0 (2020).
- 4 Zhou, Y. *et al.* Pathogenic T cells and inflammatory monocytes incite inflammatory storm in severe COVID-19 patients. *National Science Review*, doi:10.1093/nsr/nwaa041 (2020).
- 5 Xu, X., Han, Mingfeng, Li, Tiantian, Sun, Wei, Wang, Dongsheng, Fu, Binqing, Zhou, Yonggang, Zheng, Xiaohu, Yang, Yun, Li, Xiuyong, Zhang, Xiaohua, Pan, Aijun, Wei, Haiming. Effective Treatment of Severe COVID-19 Patients with Tocilizumab. [*ChinaXiv:202003.00026*] (2020).
- 6 Zumla, A., Hui, D. S., Azhar, E. I., Memish, Z. A. & Maeurer, M. Reducing

- 467 mortality from 2019-nCoV: host-directed therapies should be an option. *Lancet*
468 **395**, e35-e36, doi:10.1016/S0140-6736(20)30305-6 (2020).
- 469 7 Chaofu Wang, J. X., Lei Zhao et al. Avelar Macrophage Activation and
470 Cytokine Storm in the Pathogenesis of Severe COVID-19. *PREPRINT (Version*
471 *1) available at Research Square* [[+https://doi.org/10.21203/rs.3.rs-19346/v1](https://doi.org/10.21203/rs.3.rs-19346/v1)+]
472 (2020).
- 473 8 Li, G. *et al.* Coronavirus infections and immune responses. *J Med Virol* **92**, 424-
474 432, doi:10.1002/jmv.25685 (2020).
- 475 9 Huang, C. *et al.* Clinical features of patients infected with 2019 novel
476 coronavirus in Wuhan, China. *Lancet* **395**, 497-506, doi:10.1016/S0140-
477 6736(20)30183-5 (2020).
- 478 10 Kotch, C., Barrett, D. & Teachey, D. T. Tocilizumab for the treatment of
479 chimeric antigen receptor T cell-induced cytokine release syndrome. *Expert Rev*
480 *Clin Immunol* **15**, 813-822, doi:10.1080/1744666X.2019.1629904 (2019).
- 481 11 Le, R. Q. *et al.* FDA Approval Summary: Tocilizumab for Treatment of
482 Chimeric Antigen Receptor T Cell-Induced Severe or Life-Threatening
483 Cytokine Release Syndrome. *Oncologist* **23**, 943-947,
484 doi:10.1634/theoncologist.2018-0028 (2018).
- 485 12 Zheng, G. X. *et al.* Massively parallel digital transcriptional profiling of single
486 cells. *Nat Commun* **8**, 14049, doi:10.1038/ncomms14049 (2017).
- 487 13 Butler, A., Hoffman, P., Smibert, P., Papalexi, E. & Satija, R. Integrating single-
488 cell transcriptomic data across different conditions, technologies, and species.
489 *Nat Biotechnol* **36**, 411-420, doi:10.1038/nbt.4096 (2018).
- 490 14 Norelli, M. *et al.* Monocyte-derived IL-1 and IL-6 are differentially required for
491 cytokine-release syndrome and neurotoxicity due to CAR T cells. *Nat Med* **24**,
492 739-748, doi:10.1038/s41591-018-0036-4 (2018).
- 493 15 Aibar, S. *et al.* SCENIC: single-cell regulatory network inference and clustering.
494 *Nat Methods* **14**, 1083-1086, doi:10.1038/nmeth.4463 (2017).
- 495 16 Vento-Tormo, R. *et al.* Single-cell reconstruction of the early maternal-fetal
496 interface in humans. *Nature* **563**, 347-353, doi:10.1038/s41586-018-0698-6
497 (2018).
- 498 17 Guan, W. *et al.* Clinical Correlations of Transcriptional Profile in Patients
499 Infected With Avian Influenza H7N9 Virus. *J Infect Dis* **218**, 1238-1248,
500 doi:10.1093/infdis/jiy317 (2018).
- 501 18 Wang, Z. *et al.* Recovery from severe H7N9 disease is associated with diverse
502 response mechanisms dominated by CD8(+) T cells. *Nat Commun* **6**, 6833,
503 doi:10.1038/ncomms7833 (2015).
- 504 19 Thevarajan, I. *et al.* Breadth of concomitant immune responses prior to patient
505 recovery: a case report of non-severe COVID-19. *Nature Medicine*,
506 doi:10.1038/s41591-020-0819-2 (2020).
- 507 20 Braciale, T. J., Sun, J. & Kim, T. S. Regulating the adaptive immune response
508 to respiratory virus infection. *Nat Rev Immunol* **12**, 295-305,

509 doi:10.1038/nri3166 (2012).

510 21 Rouse, B. T. & Sehrawat, S. Immunity and immunopathology to viruses: what
511 decides the outcome? *Nat Rev Immunol* **10**, 514-526, doi:10.1038/nri2802
512 (2010).

513 22 Ahn, S. S. *et al.* Safety of Tocilizumab in Rheumatoid Arthritis Patients with
514 Resolved Hepatitis B Virus Infection: Data from Real-World Experience. *Yonsei*
515 *Med J* **59**, 452-456, doi:10.3349/ymj.2018.59.3.452 (2018).

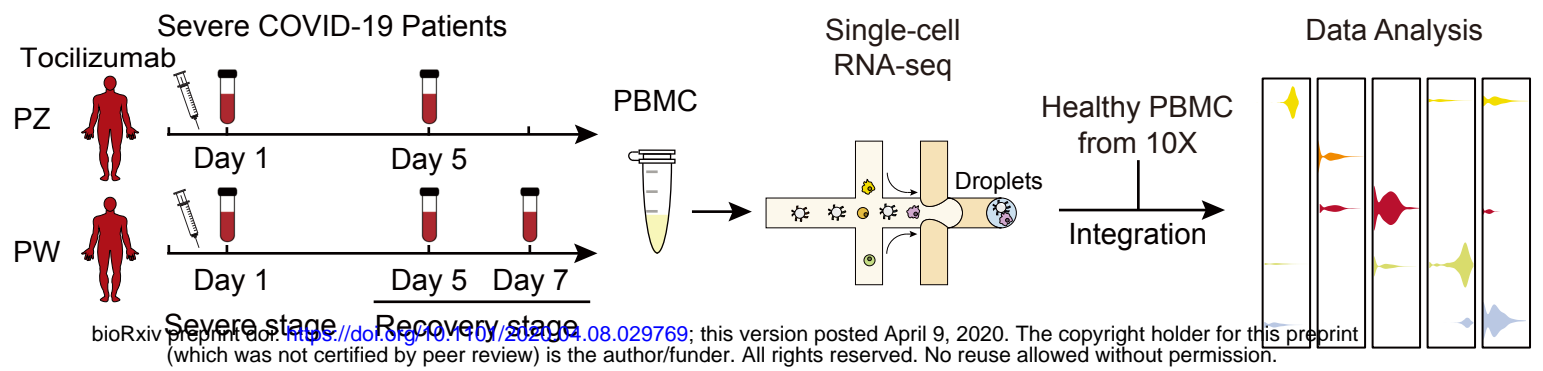
516 23 Bersanelli, M. Controversies about COVID-19 and anticancer treatment with
517 immune checkpoint inhibitors. *Immunotherapy*, doi:10.2217/imt-2020-0067
518 (2020).

519 24 Zhou, Y. *et al.* Metascape provides a biologist-oriented resource for the analysis
520 of systems-level datasets. *Nat Commun* **10**, 1523, doi:10.1038/s41467-019-
521 09234-6 (2019).

522 25 Cline, M. S. *et al.* Integration of biological networks and gene expression data
523 using Cytoscape. *Nat Protoc* **2**, 2366-2382, doi:10.1038/nprot.2007.324 (2007).

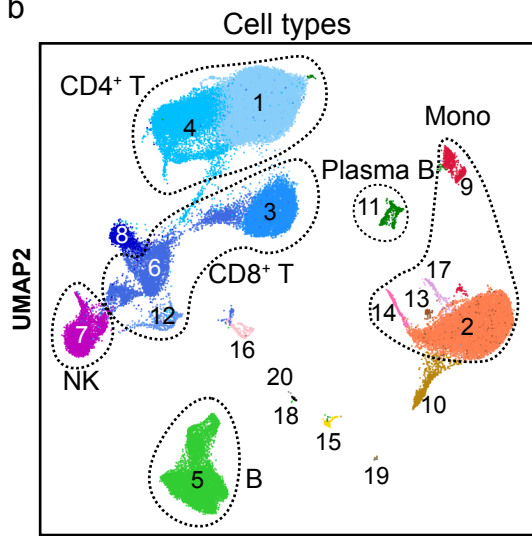
Figure 1

a



bioRxiv preprint doi: <https://doi.org/10.1101/2020.04.08.029769>; this version posted April 9, 2020. The copyright holder for this preprint (which was not certified by peer review) is the author/funder. All rights reserved. No reuse allowed without permission.

b

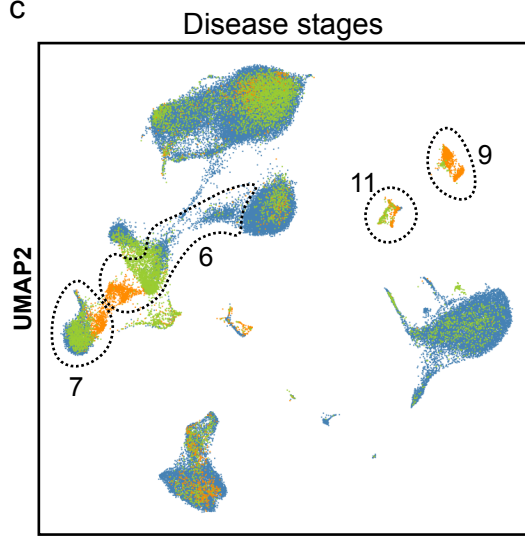


UMAP1

A UMAP plot titled "UMAP1" showing various cell clusters. The clusters are represented by numbered circles of different colors. A vertical red line separates clusters 2, 9, 13, 17, and 14 on the left from the others. Clusters 1, 4, 3, 6, and 12 are grouped under the label "Mono". Other clusters are labeled with their corresponding marker names: 8 (γδT), 7 (NK), 5 (B), 11 (Plasma B), 10 (mDC), 15 (pDC), 16 (Platelet), 18 (Progenitor), and 19 (Unknown). Cluster 20 is also present but unlabeled.

Cluster Number	Marker / Label
2	
9	
13	Mono
17	
14	
1	
4	CD4 ⁺ T
3	
6	CD8 ⁺ T
12	
8	γδT
7	NK
5	B
11	Plasma B
10	mDC
15	pDC
16	Platelet
18	Progenitor
19	Unknown
20	

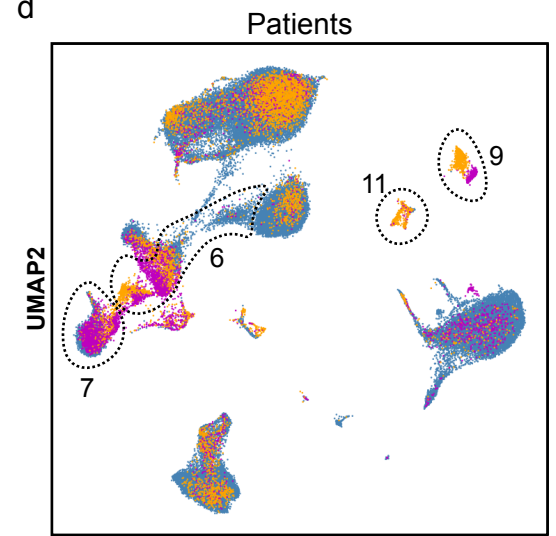
C



UMAP1

- Severe stage
- Recovery stage
- Healthy controls

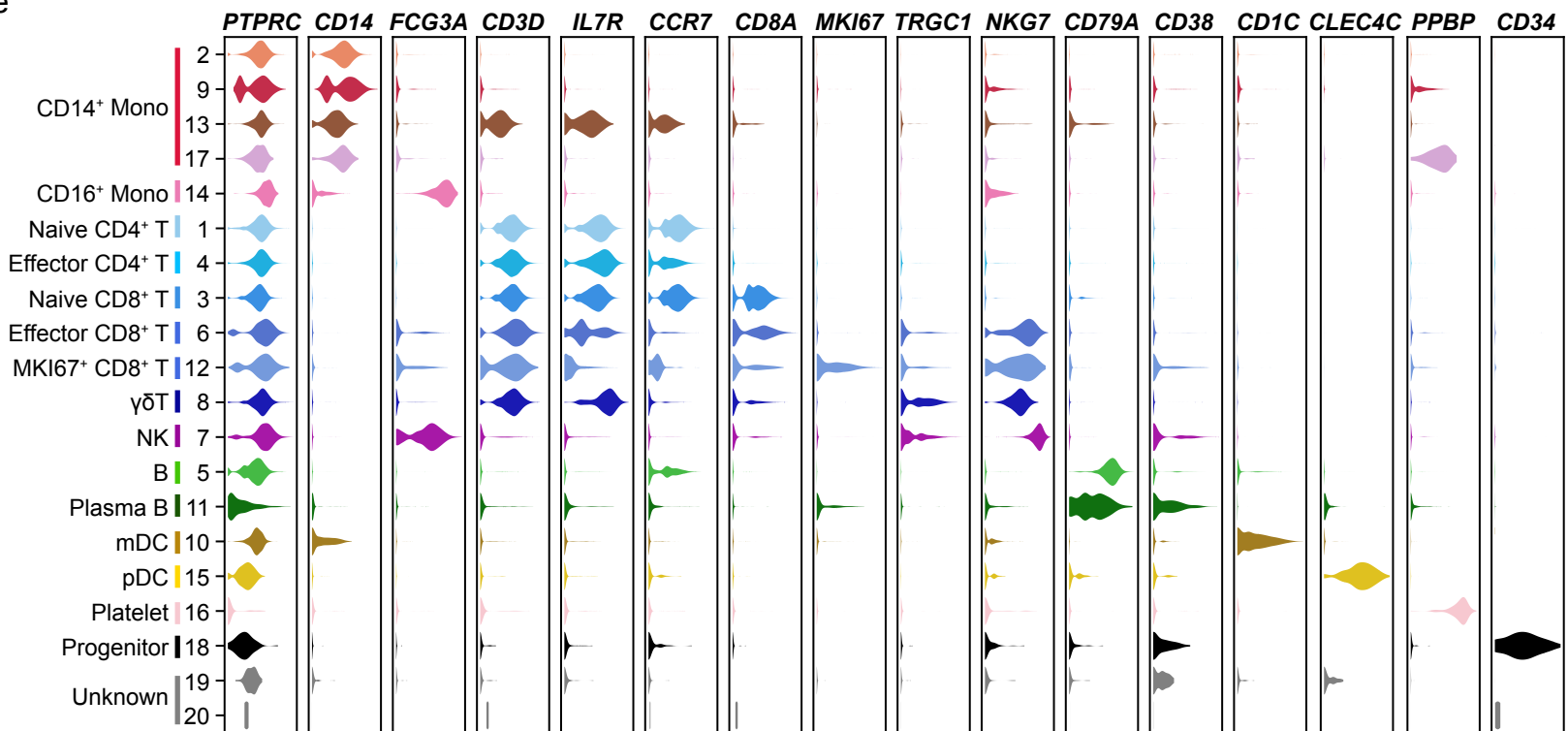
d



UMAP1

- Patient PW
- Patient PZ
- Healthy controls

e



f

